NASA Contractor Report 172545

PRELIMINARY REPORT ON TESTS OF TENS...
SPECIMENS WITH A PART-THROUGH SURFACE
NOTCH FOR A FILAMENT WOUND
GRAPHITE/EPOXY MATERIAL

C. E. Harris and D. H. Morris

VIRGINIA POLYTECHNIC INSTITUTE
AND STATE UNIVERSITY
Blacksburg, Virginia

Grant NAG1-343
March 1985

National Aeronautics and
Space Administration

Langley Research Center
Hampton, Virginia 23665

TABLE OF CONTENTS

LIST OF FIGURES

LIST OF TABLES

LIST OF SYMBOLS

a	flaw depth
B	plate half-width
c	flaw half-length at surface
E_x	laminate stiffness modulus in loading direction
E_y	laminate stiffness modulus in transverse direction
F_s	boundary-correction factor
G_{xy}	laminate shear modulus
K_I	stress intensity factor
K_Q	critical stress intensity factor
P	applied tensile load
Q	shape factor for an elliptical crack
Q_c	general fracture-toughness parameter
S	remote uniform tensile stress
t	thickness of specimen
ε_{tuf}	fiber failing strain
ν_{xy}	laminate Poisson's ratio
ξ_1	material constant
ϕ	parametric angle of the ellipse
σ_N	notched strength
σ_o	unnotched strength
$\hat{\sigma}_o$	laminate unnotched strength

ABSTRACT

The behavior of tensile coupons with surface notches of various semi-elliptical shapes has been evaluated for specimens obtained from a filament wound graphite/epoxy cylinder. The quasi-static test results in some instances are inadequate for defining complete trend curves and the interpretive analysis is considered to be preliminary. Specimens with very shallow notches were observed to be notch insensitive and the unnotched strength from these specimens was determined to be 54.97 Ksi. The failure strain of the laminate was found to be 1.328%.

Specimens with deeper notches were sensitive to notch depth, notch aspect ratio and specimen width. Using the unnotched strength of 54.97 Ksi and Poe's general toughness parameter the fracture toughness was estimated to be 27.2 Ksi $\sqrt{\text{in}}$. Isotropic linear elastic fracture mechanics together with the estimated fracture toughness correctly predicted the influence of notch depth, aspect ratio and specimen finite width.

1.0 INTRODUCTION

Damage tolerance and notched strength is of considerable interest and concern to those involved in the design and analysis of laminated or filament wound composite structures. The damage tolerance of thick filament wound cylindrical structures when subjected to foreign object impact is the subject of a joint research program conducted by NASA Langley Research Center and Virginia Polytechnic Institute and State University. The first objective of the research program is to study the development of damage due to impact and the fracture processes thereafter. The second objective is to establish impact damage analysis procedures along with a partial design data base.

Fracture mechanics based analytical procedures for structures containing a part-through semi-elliptic surface flaw are well established for evaluating surface damage in metallic structures. Because of the geometric similarity between a part-through surface flaw (or machined surface notch) and impacted surface damage in a thick laminated composite, it was postulated by the writers that the established fracture mechanics procedures might be applicable to the analysis of thick composite structures. Therefore, part of the research program involves an attempt to correlate the strength of tensile specimens with impact damage to the strength of specimens with a machined semi-elliptic part-through surface flaw.

The experimental evaluation of the fracture of tensile specimens with part-through semi-elliptic surface flaws is being conducted at Virginia Tech. Test variables include: (1) flaw depth-to-specimen thickness ratio (a/t), (2) flaw aspect ratio (a/c, where 2c is the length of the flaw at the specimen surface) and (3) specimen width

(2B). The flaw depths vary from very shallow (a/t = 0.0446) to very deep (a/t = 0.491) while the aspect ratios vary from 0.175 to 2.0. (The 0.175 aspect ratio corresponds to a 10° ellipse and the 0.5 and 2.0 ratios correspond to a 30° ellipse with the major axis parallel and normal to the specimen face, respectively.) The first phase of the test program has been completed. Test results are documented herein along with the preliminary evaluation and interpretation of the data.

2.0 EXPERIMENTAL PROGRAM

2.1 Material and Specimen Type

Test specimen coupons (2 in. x 12 in.) were obtained from a prototype graphite/epoxy filament wound cylinder prepared by Hercules Incorporated. The cylinder was 1.4 in. thick and the nonsymmetric stacking (winding) sequence is shown in Table 1. (The 0° direction is parallel to the axis of the cylinder.) The specimen coupons were cut from the cylinder with the major axis of the specimen parallel to the longitudial axis of the cylinder. This resulted in straight specimens with slightly curved parallel faces. (In order to insure uniform gripping pressure during testing, aluminum spacer plates were machined with convex and concave surfaces that matched the curvature of the specimens.) The semi-elliptic part-through surface notches were cut in the outer surface of the specimens by an ultrasonic cutting tool with a 0.016 in. thick blade. The plane of the machined notch was perpendicular to the longitudinal axis of the specimen which was also the loading direction.

In the first phase of the research program, documented herein, two

replicate tests were conducted at 18 test conditions. The complete test matrix is shown in Table 2. Straight-sided 2.0 in. wide specimens (Fig. 1) were utilized when the flaws were sufficiently large so that the predicted failure load was below 120 kips. The sides of all other specimens were machined with a 9.25-in.-radius grinding wheel resulting in a tapered specimen 1.0 in. wide in the test section where the notch was cut and 2.0 in. wide in the grip (Fig. 2). One of the straight sided 2.0 in. wide specimens from each test condition was instrumented with uniaxial strain gages oriented in the longitudinal direction. The gages were located so that in-plane and through-the-thickness bending could be monitored along with the specimen failing strain. The strain gages were located midway between the plane of the surface notch and the spacer plate (grip), as shown in Fig. 1. (A simplified finite element analysis indicated that this strain gage location was in a uniform stress region.)

2.2 Test Procedure

The quasi-static tensile tests were conducted with a hydraulic testing machine that had a 120 kip load limit. All usual equipment calibration procedures were employed. Tests were conducted at a constant crosshead displacement rate of approximately 0.10 in./min. The load was applied by wedge-action friction grips. As was previously mentioned, aluminum spacers with machined surfaces that matched the curvature of the specimens were situated between the gripping surfaces of the wedges and the specimen. The spacers were 4.0 in. long and left an unloaded specimen gage length of 4.0 in.

2.3 Data Reduction and Analysis Procedures

The load to failure was recorded in all tests. The crack-opening displacement (COD) and strain were also recorded during selected tests. The data reported herein is in terms of notched and unnotched strength rather than fracture toughness. Notched strength (σ_N) was defined as the gross far field stress at fracture and was computed by

$$\sigma_N = \frac{P}{2Bt}$$

where P = load at fracture, 2B = specimen width, and t = specimen thickness (a nominal thickness of 1.4 in. was used in all calculations).

The unnotched strength (σ_o) was determined from those specimens where the fracture was unrelated to the flaw. In those cases the unnotched strength was calculated two ways. First, the unnotched strength was calculated as the far field gross stress just like notched strength, that is, $\sigma_o = P/2Bt$. Second, unnotched strength was calculated by using the net section area as given by

$$\sigma_O = \frac{P}{2B(t-a)}$$

where a is the flaw depth. The appropriate expression for unnotched strength depended on the specimen failure mode and will be discussed in more detail in the following section.

3.0 TEST RESULTS

The notched strength test results are tabulated in Tables 3 to 6 for flaw aspect ratios 2.0, 1.0, 0.5 and 0.175 respectively. Each table includes the measured thickness, notched layer failure load, notched

strength and ratio of notched to unnotched strength for each of the two replicate tests conducted for each notch geometry. Each of the above entries in the tables will be discussed below.

The specimen length, width and notch shape were measured and recorded along with the specimen thickness prior to testing. The measured dimensions were all found to be within acceptable machining tolerances of the required dimensions and are not reported herein. Nominal dimensions were used in all calculations. The tabulated thickness value for each specimen is the average of three readings taken at the notch and midway along the specimen length in each direction from the notch. (As previously stated, a nominal thickness of 1.4 in. was used in all calculations).

The specimens failed according to two distinct failure processes depending on the notch geometry. The specimens with shallow notches ($a/t < 0.1$) failed in a catastrophic manner. However, the specimens with deeper notches ($a/t > 0.1$) exhibited a distinct two-part fracture. The first fracture produced a long delamination at the bottom of the notch running completely across the specimen width and for 2.0 in. to 4.0 in. along the specimen length in both directions from the notch. (This is shown by the X-ray radiograph in Fig. 3.) The specimen also fractured across the width from the notch to the edge. There was no apparent damage to the layer below the notch. This fracture process is referred to as the notched layer failure. The notched layer failure was associated with a reduction in the applied load. The specimen was then reloaded to obtain the unnotched layer failure load. The load tabulated in Tables 3-6 is the load at which the notched layer failed or the catastrophic failure load of the specimen whichever occurred

first. The notched strength σ_N was then calculated by the first failure load with the procedure described in Article 2.3, that is, $\sigma_N = P/2Bt$.

The catastrophic failure of the specimens with the very shallow notch ($a/t < 0.1$) was in general not directly influenced by the presence of the notch. All the specimens with shallow notches were tapered down to a 1.0 in. wide test section at the notch. Failure did occur in the test section. However, the catastrophic failures were splintered similar to tensile failures of laminated composites (see Fig. 4). Oftentimes a surface layer or splinter would contain the entire notch completely intact (see Fig. 4). Because of this obvious notch insensitivity, the strength of these specimens was taken to be the unnotched strength σ_o of the filament wound cylinder. These values of unnotched strength are tabulated in Table 7, where unnotched strength has been calculated by both procedures outlined in Article 2.3. Using the full cross-sectional area of the specimen, the mean value of strength was 52.00 Ksi with a standard deviation of 3.30 Ksi for the 18 tests. Alternatively, using the net section area resulted in a slightly higher mean value of 54.97 Ksi but a lower standard deviation of 2.80 Ksi. Because of the lower standard deviation the unnotched strength will be taken as $\hat{\sigma}_o = 54.97$ Ksi.

For those specimens that exhibited a two-part fracture, the unnotched strength can be approximated from the failure of the unnotched layer. Basing the calculations on the net section area (area of the layer below the bottom of the notch), values of unnotched strength σ_o are tabulated in Table 8. The values are segregated by specimen width (this does not imply that there is a specimen width effect). Based on 5 test values for each width, the values of unnotched

strength (standard deviation) are 56.63 Ksi (3.13 Ksi) and 62.15 Ksi (4.58 Ksi) for a specimen width of 1.0 in. and 2.0 in., respectively. The strength of the unnotched layer of specimens with a 1.0 in. wide test section was very close to the strength of the similar specimens that failed catastrophicaly. However, the strength of the unnotched layers in the 2.0 in. wide specimens was about 10% higher.

As previously mentioned five specimens were instrumented with uniaxial strain gages to measure the laminate failing strain and to check for in-plane (width) and through-the-thickness bending. Only the straight-sided 2.0 in. wide specimens were instrumented with gages. The values of laminate failure strain are presented in Table 9. With a total of 10 gages operational at catastrophic fracture of the unnotched layer, the mean value of laminate failure strain was 1.328% with a standard deviation of 0.035%. Initial strain gage values of inplane bending differed by 0%-14%. Through-the-thickness strain gage readings differed by 6%-25%, being higher for deeper notches.

4.0 INTERPRETATION AND DISCUSSION OF RESULTS

The analytical isotropic solutions for the semi-elliptic surface crack generated by Newman and Raju [1] will be utilized to aid in the interpretation of the experimental results. Reference 1 provides empirical stress-intensity factor equations for a three dimensional finite-element analysis of the cracked-body geometry. The stress-intensity factor equations are a function of the parametric angle of the ellipse (ϕ), flaw depth (a), flaw length (2c), plate thickness (t), and plate width (2B), as shown in Fig. 1. Written symbolically, the stress intensity factor is given by [1],

$$K_I = S \left(\pi \frac{a}{Q}\right)^{1/2} F_s\left(\frac{a}{c}, \frac{a}{t}, \frac{c}{B}, \phi\right) \qquad (1)$$

where S = remote uniform tensile stress and Q = ellipse shape factor, $Q = Q(\frac{a}{c})$.

In fracture mechanics terminology, the value of the stress-intensity factor at fracture is typically referred to as the critical stress-intensity factor (K_Q) or fracture toughness. If the fracture toughness of the material is known, equation 1 can be rewritten to provide the remote stress at failure (notched strength) for a given flaw geometry. The predicted notched strength is then given by

$$\sigma_N = \frac{K_Q}{(\frac{\pi a}{Q})^{1/2} F_s} \quad . \tag{2}$$

In the absense of a measured value of fracture toughness, a design value was estimated from Poe's general toughness parameter model [2] developed for laminated composites. The general toughness parameter, which was found to be relatively constant for all laminates, is given by

$$\frac{Q_c}{\epsilon_{tuf}} = 1.5 \sqrt{mm} \tag{3}$$

where $Q_c = K_Q \, \xi_1 / E_X$

K_Q = stress intensity factor at failure

$\xi_1 = 1 - \nu_{xy} \left(\frac{E_y}{E_x} \right)^{1/2}$

E_x = laminate stiffness modulus in loading direction

E_y = laminate stiffness modulus in transverse inplane direction

ν_{xy} = laminate inplane Poisson's ratio

ε_{tuf} = fiber failing strain.

The laminate engineering stiffness constants were determined to be

$$E_x = 4.442 \times 10^6 \text{ psi}$$
$$E_y = 5.656 \times 10^6 \text{ psi}$$
$$G_{xy} = 2.862 \times 10^6 \text{ psi}$$
$$\nu_{xy} = 0.3509$$
$$\xi_1 = 0.6040$$

These properties were calculated using laminate theory from lamina properties supplied by Hercules Incorporated. The laminate was assumed symmetric to represent the rigid grips, which allow little or no bending. (The cylinder with internal pressure also has no bending). Since the laminate stress-strain behavior was essentially linear to failure, the fiber failing strain was estimated from the unnotched strength as follows:

$$\varepsilon_{tuf} = \frac{\hat{\sigma}_o}{E_x} = \frac{54.97 \times 10^3}{4.442 \times 10^6} = 0.0124 \ .$$

Finally, using equation 3 the fracture thoughness was estimated to be 27.2 Ksi $\sqrt{\text{in.}}$.

Predicted values of notched strength using equation 2 with K_Q = 27.2 Ksi $\sqrt{\text{in.}}$ are compared to the experimental values in Figs.

5-7 for notch aspect ratios 2.0, 1.0 and 0.5, respectively. For a given notch, the value of F_s depends on ϕ. The maximum value, which occurs at ϕ = 0° or 90° depending on notch shape, was used in the calculations with equation (2), just like in metals. The values of ϕ for maximum F_s are shown in Figs. 5-7 for each flaw shape. Normalized notched strength ($\sigma_N/\hat{\sigma}_0$ where $\hat{\sigma}_0$ = 54.97 Ksi) versus notch depth-to-thickness is plotted for the various flaw aspect ratios (a/c). The horizontal line drawn at $\sigma_N/\hat{\sigma}_0$= 1 indicates that the notched strength cannot exceed the unnotched strength.

The comparisons in Figs. 5-7 clearly show two distinct regions of behavior. Shallow notches are governed by the unnotched strength which is often times referred to as net section ultimate. Deeper notches are influenced by both notch depth (a) and notch aspect ratio (a/c). For deeper notches isotropic linear elastic fracture mechanics appears to accurately predict the influence of notch shape and size as well as the specimen finite width effect. The data in Fig. 5 for a/c = 2.0 are sufficient to show the nature of the transition from behavior governed by net section ultimate to that governed by fracture mechanics. However, additional data is needed for the other flaw shapes to show the transition. (It should be noted that the above described behavior of the filament wound material is very similar to the typical behavior of isotropic metals under the influence of surface flaws.)

5.0 SUMMARY AND CONCLUSIONS

The behavior of tensile coupons under quasi-static loading with various surface notch geometries has been evaluated for specimens obtained from a filament wound graphite/epoxy cylinder. Specimens with very shallow notches were observed to be notch insensitive and the

unnotched strength from these specimens was determined to be 54.97 Ksi. From 5 instrumented specimens and 10 active gages at failure, the failure strain of the laminate was found to be 1.328%. Specimens with deeper notches were sensitive to notch depth, notch aspect ratio and specimen width.

A value of fracture toughness was estimated to be 27.2 Ksi$\sqrt{\text{in}}$. based on the above value of unnotched strength and Poe's general toughness parameter for laminated composites. Using this value of fracture toughness and isotropic linear elastic fracture mechanics, the influence of notch depth, aspect ratio and specimen finite width was correctly predicted for deep flaws.

The general conclusion reached from this study is that the behavior of the filament wound graphite/epoxy material is similar to that for an isotropic metal under the influence of semi-elliptic surface flaws. The failure of specimens with shallow notches is governed by net section ultimate whereas failure of specimens with deeper notches is governed by fracture mechanics. The transition region between the two behavior extremes was not adequately defined by this test program for all the flaw shapes investigated. A complete trend curve only exists for a notch aspect ratio of 2.0.

REFERENCES

1. Newman, J. C., Jr., and Raju, I.S., "Stress-Intensity Factor Equations for Cracks in Three-Dimensional Finite Bodies," Fracture Mechanics: Fourteenth Symposium - Volume I: Theory and Analysis, ASTM STP 791, J. C. Lewis and G. Sines, Eds., American Society for Testing and Materials, 1983, pp. I-238-I-265.

2. Poe, Jr., C. C., "A Unifying Strain Criterion for Fracture of Fibrous Composite Laminates," Engineering Fracture Mechanics, Vol. 17, 1983, p. 153-171.

Table 1 Cylindrical Stacking (Winding) Sequence

Inside Surface	± 90°	fabric weave, 0.01683 in.
	2 @ ∓ 56.45°	double helical winding, 0.06732 in.[a]
	2 @ 0°	6 plies of tape, hand layup, 0.03366 in
	∓ 56.45°	single helical winding, 0.03366 in.[a]
	2 @ 0°	
	∓ 56.45°	
	2 @ 0°	
	∓ 56.45°	
	2 @ 0°	
	∓ 56.45°	
	0°	3 plies of tape, hand layup, 0.01683 in.
	2 @ ∓ 56.45°	
	0°	
	2 @ ∓ 56.45°	
	0°	
	2 @ ∓ 56.45°	
	0°	
	2 @ ∓ 56.45°	
	0°	
	2 @ ∓ 56.45°	
	0°	
	2 @ ∓ 56.45°	
	0°	
	2 @ ∓ 56.45°	
	0°	
	2 @ ∓ 56.45°	cut double helical winding, (0.11216 in.[b])
	0°	
	2 @ ∓ 56.45°	
	0°	
Outside Surface	2 @ ∓ 56.45°	

Notes:

[a] 24.3 tows/inch/layer

[b] 38.7 tows/inch/layer

Table 2 Specimen Test Matrix

a/c = 2.0		a/c = 1.0		a/c = 0.5		a/c = 0.175	
a/t	2B (in.)	a/t	2B (in.)	a/t	2B (in.)	a/t	2B (in.)
0.0670	1.0	0.0335	1.0	0.0558	1.0	0.0335	1.0
0.123	1.0	0.0446	1.0	0.0670	1.0	0.0446	1.0
0.179	1.0	0.0558	1.0	0.123	1.0		
0.290	1.0	0.290	2.0	0.179	2.0		
0.402	1.0	0.402	2.0				
0.491	2.0	0.491	2.0				

Table 3 Experimental Data for a/c = 2.0

a/t	Specimen ID	Thickness (in.)	2B (in.)	Failure Load (Kips)	σ_N^1 Ksi	$\sigma_N / \hat{\sigma}_0$
0.0670	2-7	1.403	1.0	74.2	53.0	0.964
	2-8	1.400		73.2	52.3	0.951
		Average		73.7	52.7	0.959
0.123	2-13	1.401	1.0	67.6	48.3	0.879
	2-14	1.402		67.4	48.1	0.875
		Average		67.5	48.2	0.877
0.179	2-28	1.398	1.0	61.0	43.6	0.793
	2-29	1.401		62.6	44.7	0.813
		Average		61.8	44.1	0.802
0.290	2-30	1.403	1.0	43.2	30.9	0.562
	2-31	1.401		47.0	33.6	0.611
		Average		45.1	32.3	0.588
0.402	2-36	1.398	1.0	37.8	27.0	0.491
	2-37	1.401		34.8	24.9	0.453
		Average		36.3	26.0	0.473
0.491	2-45	1.399	2.0	86.5	30.9	0.562
	2-46	1.400		88.2	31.5	0.573
		Average		87.4	31.2	0.568

1 $\sigma_N = P/1.4(2B)$

Table 4 Experimental Data for a/c = 1.0

a/t	Specimen ID	Thickness (in.)	2B (in.)	Failure Load (Kips)	σ_N^1 (Ksi)	$\sigma_N/\hat{\sigma}_O$
0.0335	2-21	1.403	1.0	77.5	55.4	1.008
	2-22	1.397		73.2	52.3	0.951
		Average		75.4	53.9	0.981
0.0446	2-23	1.406	1.0	76.1	54.4	0.990
	2-26	1.402		80.6	57.6	1.048
		Average		78.4	56.0	1.019
0.0558	2-27	1.400	1.0	73.7	52.6	0.957
	2-34	1.400		75.4	53.9	0.981
		Average		74.6	53.3	0.970
0.290	2-12	1.398	2.0	87.8	31.4	0.571
	2-40	1.398		84.8	30.3	0.551
		Average		86.3	30.9	0.562
0.402	2-41	1.398	2.0	66.4	23.7	0.431
	2-42	1.398		69.5	24.8	0.451
		Average		68.0	24.3	0.442
0.491	2-43	1.398	2.0	54.5	19.5	0.355
	2-44	1.397		50.0	17.9	0.326
		Average		52.3	18.7	0.340

[1] $\sigma_N = P/1.4(2B)$

Table 5 Experimental Data for a/c = 0.5

a/t	Specimen ID	Thickness (in.)	2B (in.)	Failure Load (Kips)	σ_N^1 (Ksi)	$\sigma_N/\hat{\sigma}_0$
0.0558	2-17	1.399	1.0	66.9	47.8	0.870
	2-18	1.397		70.3	50.2	0.913
		Average		68.6	49.0	0.891
0.0670	2-19	1.403	1.0	70.0	50.0	0.910
	2-20	1.401		67.1	47.9	0.871
		Average		68.6	49.0	0.891
0.123	2-2	1.400	1.0	44.2	31.6	0.575
	2-3	1.403		40.9	29.2	0.531
		Average		42.6	30.4	0.553
0.179	2-10	1.400	2.0	86.5	30.9	0.562
	2-11	1.399		92.5	33.0	0.600
		Average		89.5	32.0	0.582

[1] $\sigma_N = P/1.4\ (2B)$

Table 6 Experimental Data for a/c = 0.175

a/t	Specimen ID	Thickness (in.)	2B (in.)	Failure Load (Kips)	σ_N^1 (Ksi)	$\sigma_N/\hat{\sigma}_0$
0.0335	2-4	1.399	1.0	68.0	48.6	0.884
	2-5	1.398		80.0	57.1	1.039
		Average		74.0	52.9	0.962
0.0446	2-9	1.396	1.0	75.2	53.7	0.977
	2-35	1.401		68.2	48.7	0.886
		Average		71.7	51.2	0.931

[1] $\sigma_N = P/1.4\ (2B)$

Table 7 Unnotched Strength from Specimens that Failed Catastrophically

SPEC ID	2B (in.)	a (in.)	Failure Load (Kips)	Unnotched Strength[1] (Ksi)	Unnotched Strength[2] (Ksi)
2-4	1.0	0.0469	68.0	48.57	50.25
2-5	1.0	0.0469	80.0	57.14	59.12
2-22	1.0	0.0469	73.2	52.29	54.10
2-21	1.0	0.0469	77.5	55.36	57.28
2-23	1.0	0.0625	76.1	54.36	56.90
2-26	1.0	0.0625	80.6	57.57	60.26
2-9	1.0	0.0625	75.2	53.71	56.22
2-35	1.0	0.0625	68.2	48.71	50.99
2-17	1.0	0.0781	66.9	47.79	50.61
2-18	1.0	0.0781	70.3	50.21	53.18
2-27	1.0	0.0781	73.7	56.64	55.75
2-34	1.0	0.0781	75.4	53.86	57.04
2-20	1.0	0.0938	67.1	47.93	51.37
2-19	1.0	0.0938	70.0	50.00	53.59
2-7	1.0	0.0938	74.2	53.00	56.81
2-8	1.0	0.0938	73.2	52.29	56.04
2-13	1.0	0.172	67.6	48.29	55.05
2-14	1.0	0.172	67.4	48.14	54.89
			Number of Tests	18	18
			Mean Value	52.00	54.97
			STD Deviation	3.30	2.80

1. $\sigma_0 = P/(1.4)2B$

2. $\sigma_0 = P/2B\ (1.4-a)$

Table 8 Unnotched Strength from the Fracture of the Unnotched Layer of Specimens with Two-Part Failures

Spec ID	2B (in.)	a (in.)	Failure Load (Kips)	Unnotched Strength[1] (Ksi)
2-2	1.0	0.172	71.0	57.82
2-3	1.0	0.172	67.2	54.72
2-29	1.0	0.250	62.6	54.43
2-31	1.0	0.406	53.6	53.92
2-36	1.0	0.563	52.1	62.25
			Average	56.63
			STD Deviation	3.13
2-40	2.0	0.406	111.5	56.09
2-42	2.0	0.563	97.7	58.36
2-44	2.0	0.689	93.4	65.68
2-45	2.0	0.689	97.5	68.57
2-46	2.0	0.689	88.2	62.03
			Average	62.15
			STD Deviation	4.58

1. $\sigma_0 = P/2B\ (1.4\text{-}a)$

Table 9 Laminate Failure Strain from 2 in. Wide Specimens

Specimen ID	a/t	Gage Location	Strain At Failure %
2-11	0.179	1	1.35
2-40	0.290	1	1.33
2-42	0.402	2	1.32
		3	1.36
		1	1.32
2-44	0.491	2	1.24
		3	1.35
		1	1.30
2-46	0.491	3	1.36
		1	1.35
		Average	1.328
		STD Deviation	0.035

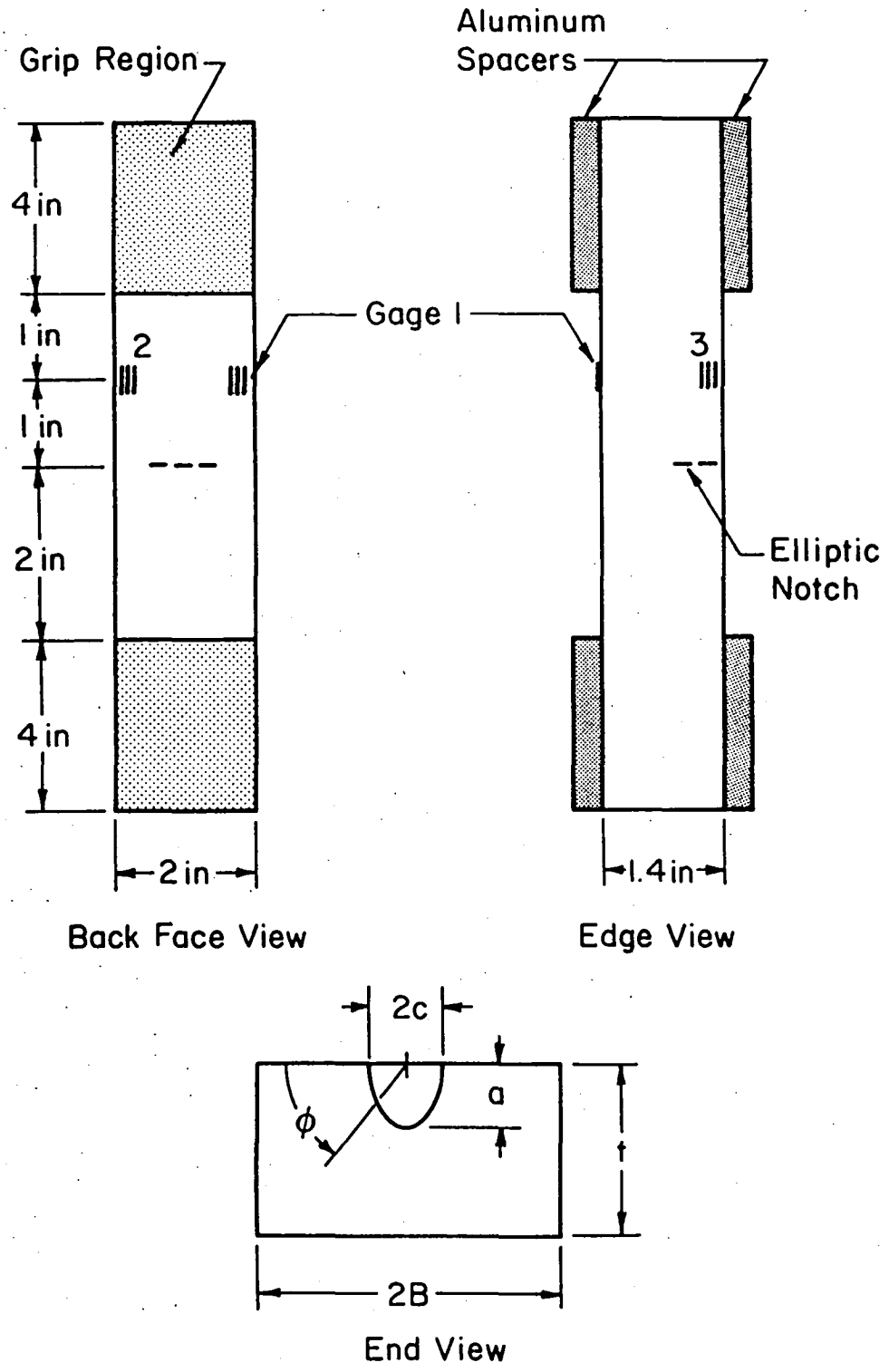

Fig. 1 Schematic of straight - sided specimen

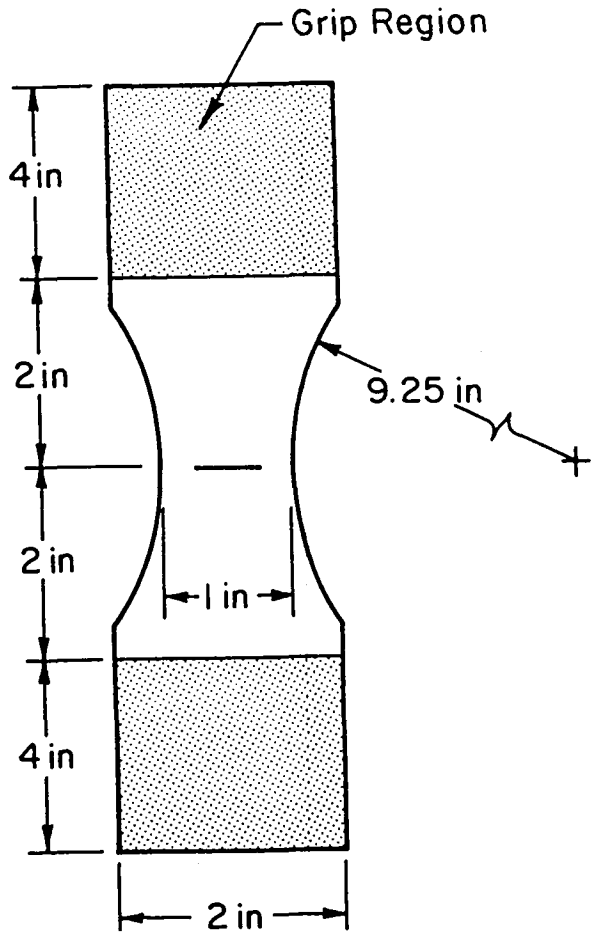

Fig. 2 Schematic of tapered specimen

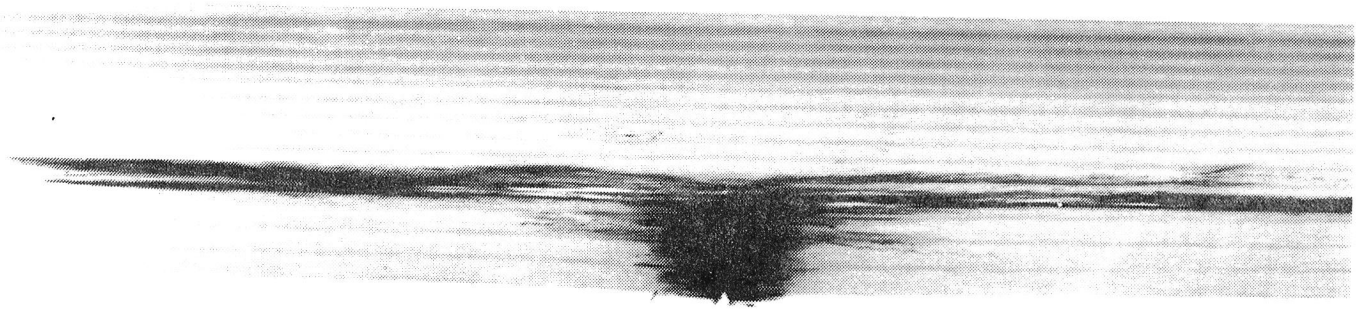

Fig. 3 Photograph of specimen showing delamination at the bottom of the notch and the fractured notched layer

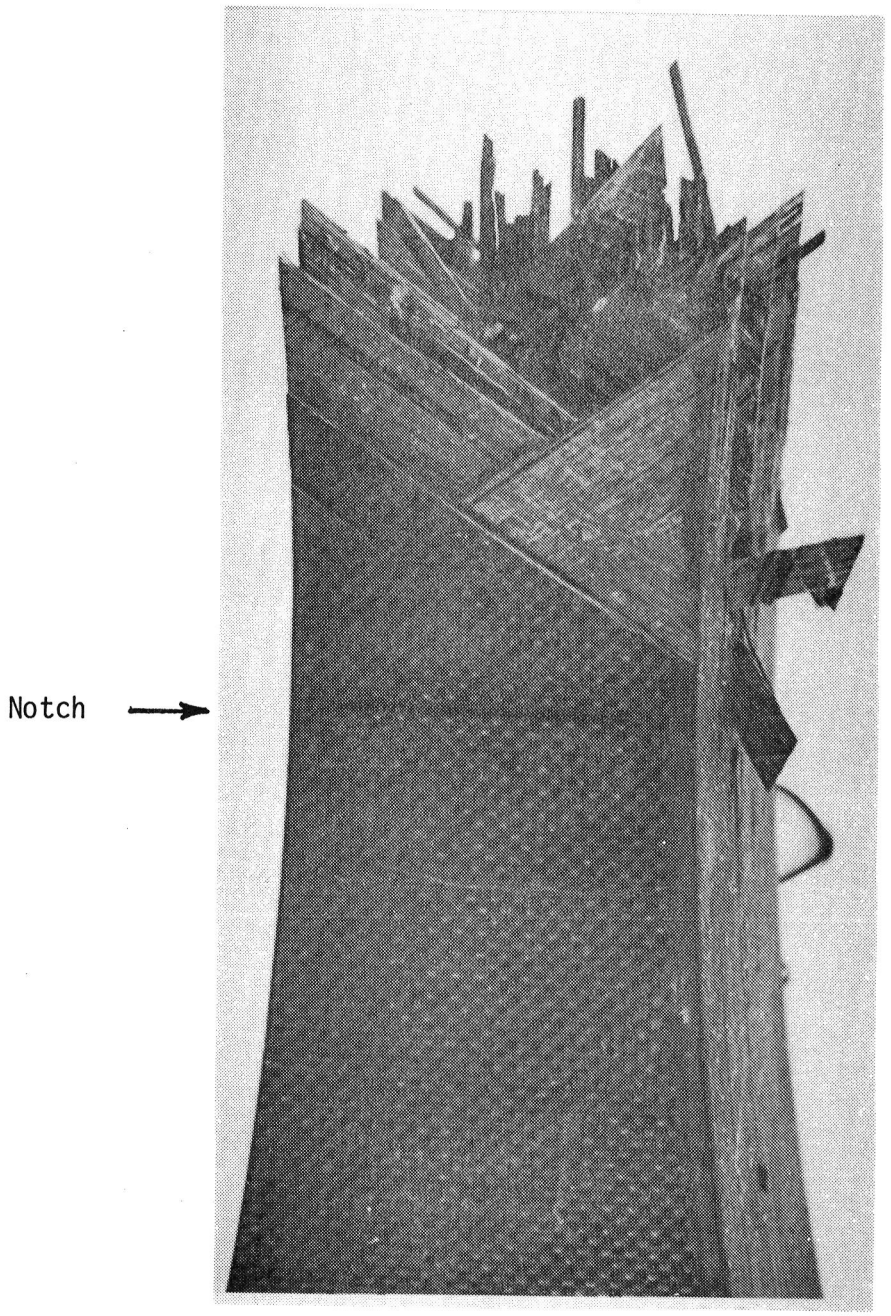

Fig. 4 Photograph of a specimen that failed catastrophically

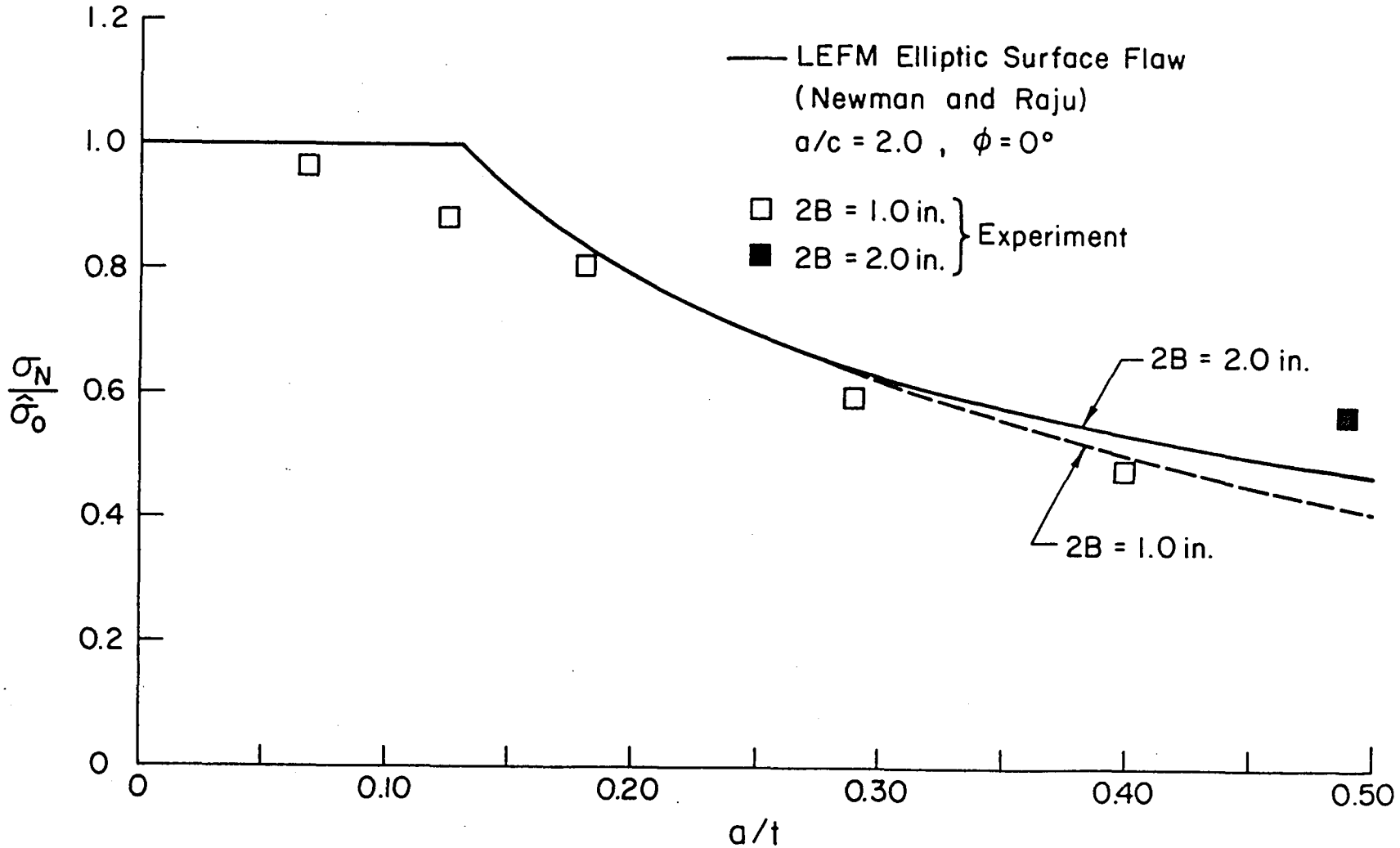

Fig. 5 Comparison of experimental data to isotropic LEFM predictions for a/c = 2.0

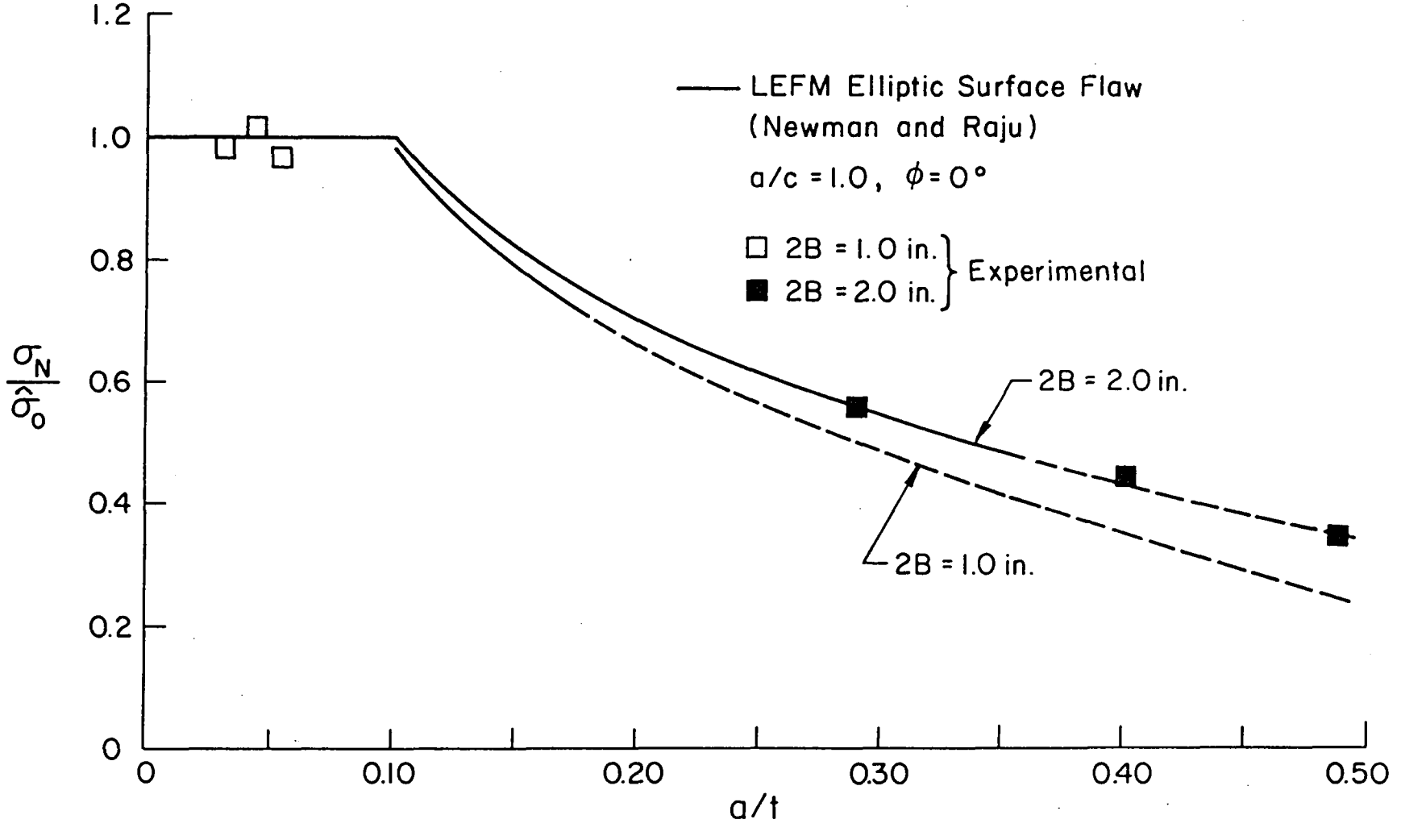

Fig. 6 Comparison of experimental data to isotropic LEFM predictions for a/c = 1.0

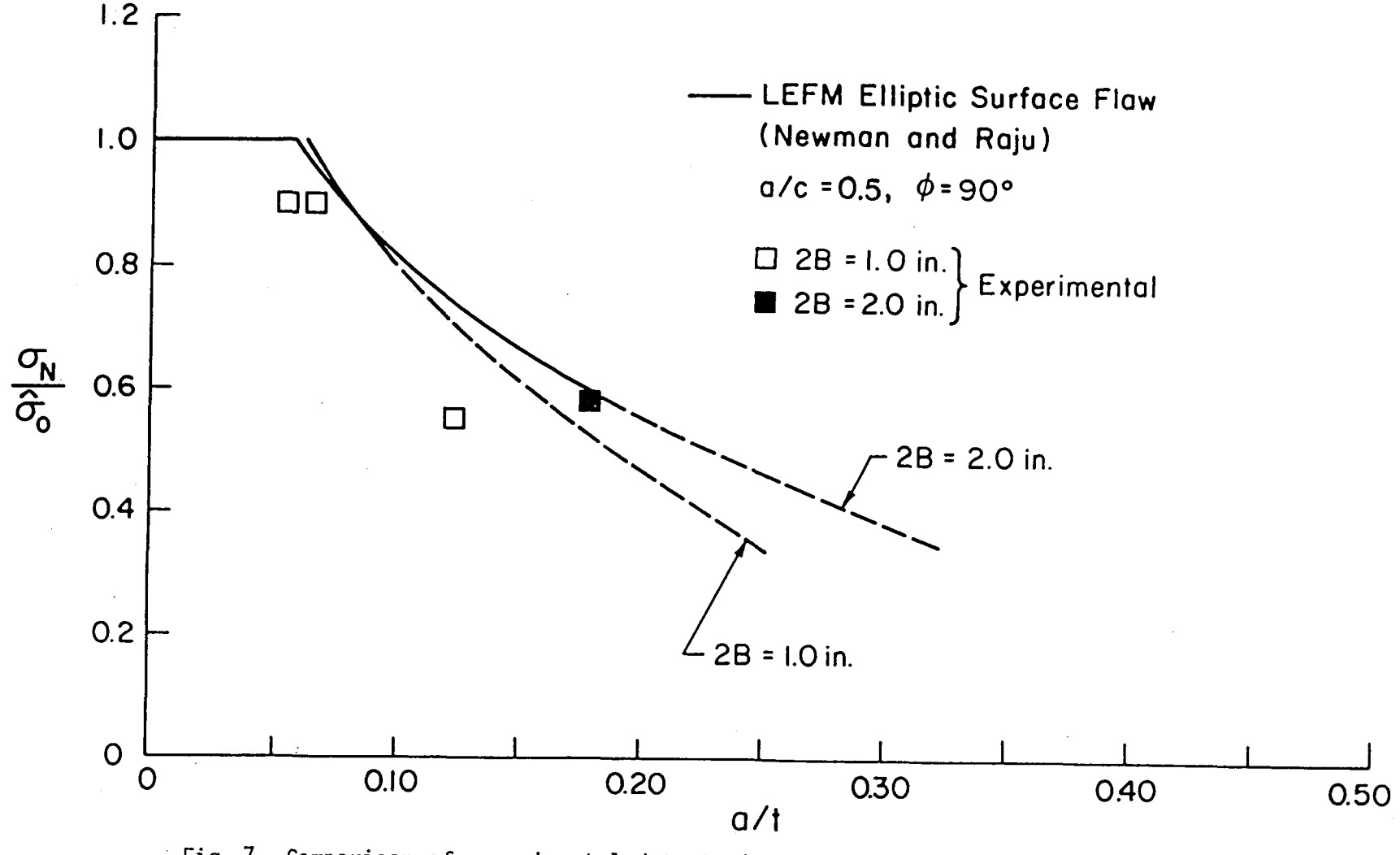

Fig. 7 Comparison of experimental data to isotropic LEFM predictions for a/c = 0.5

1. Report No.	2. Government Accession No.	3. Recipient's Catalog No.
NASA CR-172545		

4. Title and Subtitle	5. Report Date
Preliminary Report on Tests of Tensile Specimens with a Part-Through Surface Notch for a Filament Wound Graphite/Epoxy Material	March 1985
	6. Performing Organization Code
7. Author(s)	8. Performing Organization Report No.
C. E. Harris and D. H. Morris	
9. Performing Organization Name and Address	10. Work Unit No.
Virginia Polytechnic Institute and State University Engineering Science and Mechanics Department Blacksburg, VA 24061	
	11. Contract or Grant No.
	NAG1-343
12. Sponsoring Agency Name and Address	13. Type of Report and Period Covered
National Aeronautics and Space Administration Washington, DC 20546	Contractor Report
	14. Sponsoring Agency Code
	505-33-33-05

15. Supplementary Notes

Langley Technical Monitor: C. C. Poe, Jr.

16. Abstract

The behavior of tensile coupons with surface notches of various semi-elliptical shapes has been evaluated for specimens obtained from a filament wound graphite/epoxy cylinder. The quasi-static test results, in some instances, are inadequate for defining complete trend curves and the interpretive analysis is considered to be preliminary. Specimens with very shallow notches were observed to be notch insensitive and the unnotched strength from these specimens was determined to be 54.97 Ksi. The failure strain of the laminate was found to be 1.328%.

Specimens with deeper notches were sensitive to notch depth, notch aspect ratio and specimen width. Using the unnotched strength of 54.97 ksi and Poe's general toughness parameter, the fracture toughness was estimated to be 27.2 ksi $\sqrt{\text{in}}$. Isotropic linear elastic fracture mechanics together with the estimated fracture toughness correctly predicted the influence of notch depth, aspect ratio and specimen finite width.

17. Key Words (Suggested by Author(s))	18. Distribution Statement
Fracture, composites, surface crack, thick laminate	Unclassified-Unlimited Subject Category 24

19. Security Classif. (of this report)	20. Security Classif. (of this page)	21. No. of Pages	22. Price
Unclassified	Unclassified	34	A03

For sale by the National Technical Information Service, Springfield, Virginia 22161